Electronic Supplementary Material (ESI) for ChemComm.

Fluorescence-enhanced supra-amphiphilies based on pillar[5]arene: construction, controllable self-assembly and application in cell-imaging

Lizhen Fang,[a,b] Yu Dai,[b] Yiqiao Bai,[b] Yujia Meng,[b] Wenqiang Yu,[b] Yunhan Gao,[b] Ruowen Tang,[b] Yue Zhang,[b] Liang Li,*[,a] Jin Wang,[b] Yue Ding,[b] Yang Wang,[b] Tingting Chen,[b] Yan Cai,[b] and Yong Yao*[,b]

[a]*School of Chemical and Environmental Engineering, Shanghai Institute of Technology, Shanghai 201418, China.*

[b]*School of Chemistry and Chemical Engineering, Nantong University, Nantong, Jiangsu, 226019, P.R. China.*

E-mail: lilianglcx@sit.edu.cn; yaoyong1986@ntu.edu.cn.

Supporting Information (19 pages)

1. Materials and methods

Materials

All reagents were commercially available and used as supplied without further purification. Solvents were either employed as purchased or dried according to procedures described in the literature. The cell lines used in the study were purchased from Jiangsu A.K.X. Material Technology Co., Ltd.

Measurements

NMR spectroscopy. ^{1}H and ^{13}C NMR spectra were recorded on a Brucker AV400 spectrometer.

Fluorescence spectroscopy. Steady-state fluorescence spectra were recorded in a conventional quartz cell (light path 10 mm) on a Varian Cary Eclipse equipped with a Varian Cary single-cell peltier accessory to control temperature.

UV/Vis spectroscopy. UV/Vis spectra and the optical transmittance were recorded in a quartz cell (light path 10 mm) on a Shimadzu UV-3600 spectrophotometer equipped with a PTC-348WI temperature controller.

ESI-MS spectroscopy. Electrospray ionization mass spectra (ESI-MS) were measured by Agilent 6520 Q-TOF-MS.

Cytotoxicity experiments. HeLa cells were incubated in Dulbecco's modified Eagle's medium (DMEM). The medium was supplemented with 10% fetal bovine serum and 1% Penicillin-Streptomycin. Cells were seeded in 96-well plates (5×10^4 cell mL^{-1}, 0.1 mL per well) for 4 h at 37°C in 5% CO_2. Then the cells were incubated with different groups for 4 h. The relative cellular viability was determined by the MTT assay.

Confocal laser scanning microscopy. Cells were seeded in 6-well plates (5×10^4 cell mL^{-1}, 2 mL per well) for 24 h at 37°C in 5% CO_2. The cells were incubated with the corresponding solution for 4 h. Then the medium was removed, and the cells were

washed with phosphate buffer solution for three time. Finally, the cells were subjected to observation by a confocal laser scanning microscope.

TEM microscopy. High-resolution Transmission electron microscopy (TEM) images were acquired using a Tecnai 20 high-resolution transmission electron microscope operating at an accelerating voltage of 200 keV. The sample for high-resolution TEM measurements was prepared by dropping the solution onto a copper grid. The grid was then air-dried.

SEM microscopy. Scanning electron microscopy (SEM) investigations were carried out on a HitachiS-3400 SEM instrument.

DLS spectroscopy. Solution samples were examined on a laser light scattering spectrometer (BI-200SM) equipped with a digital correlator (TurboCorr) at 636 nm at a scattering angle of 90°. The hydrodynamic diameter (Dh) was determined by DLS experiments at 25°C.

2. Synthesis of $ENDT_n$

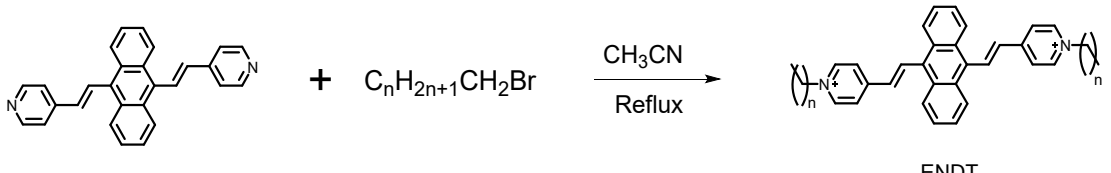

9,10-bis (e) -2- (pyridine-4-yl) vinylanthracene

n = 1, 3, 5, 9

$ENDT_n$

Scheme S1. Synthetic route to $ENDT_n$.

$ENDT_n$ was prepared successfully by refluxing compound 9,10-bis (e) -2- (pyridine-4-yl) vinylanthracene and bromo-alkanes in MeCN (30 mL). In a typical process, compound 9,10-bis (e) -2- (pyridine-4-yl) vinylanthracene (0.49 g, 1.0 mmol) and excess bromoethane (1.08 g, 10.0 mmol) were added to MeCN (30 mL) and then reflux overnight. After the reaction was finished, the reaction mixture was cold to room temperature, $ENDT_1$ was filtered off and washed with MeCN for 3 times. The yield was about 50.3%. Compound $ENDT_3$, $ENDT_5$, $ENDT_9$ are repeat by this step.

$ENDT_1$: Red solid, 56.7 %; m.p. > 250 °C. ^{1}H NMR (400 MHz, D_2O) δ (ppm): 8.68(d, 4H), 8.24(d, 2H), 8.10(m, 4H)，8.01(m, 4H), 7.46(m, 4H)，6.90(d, 2H), 4.53(t, 4H), 1.58(m, 6H). ^{13}C NMR (100 MHz, D_2O) δ (ppm): 151.8, 143.2, 136.3, 131.4, 130.5, 128.0, 126.3, 125.2, 124.1, 56.2, 15.6. LRMS spectra of $ENDT_1$. Calcd. For C32H30N2 ($[M - 2Br]^{2+}$): 221.12, found: 221.11. IR(KBr) υ: 3432, 3020, 2923, 1610, 1556, 1513, 1466, 1462, 1441, 1377, 1335, 1208, 1161, 1008, 864, 753, 710 cm^{-1}.

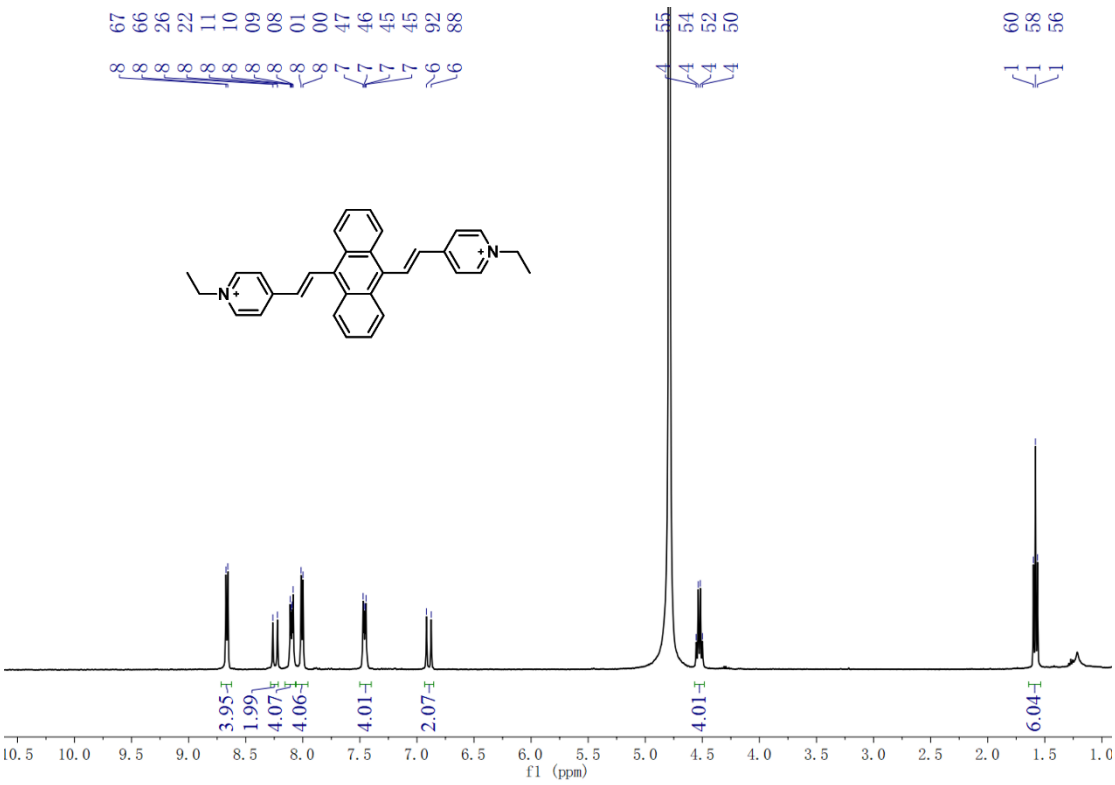

Figure S1: ^{1}H NMR spectra (400 MHz, 298 K, D_2O) of compound $ENDT_1$.

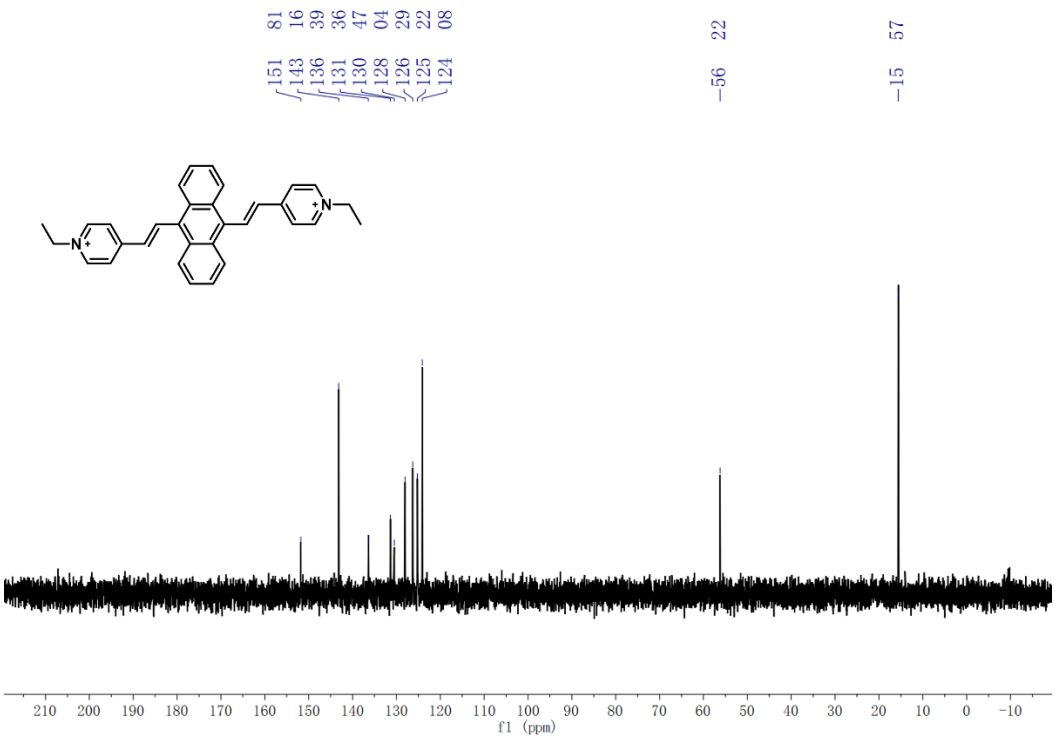

Figure S2. ^{13}C NMR spectra (100 MHz, 298 K, D_2O) of compound $ENDT_1$.

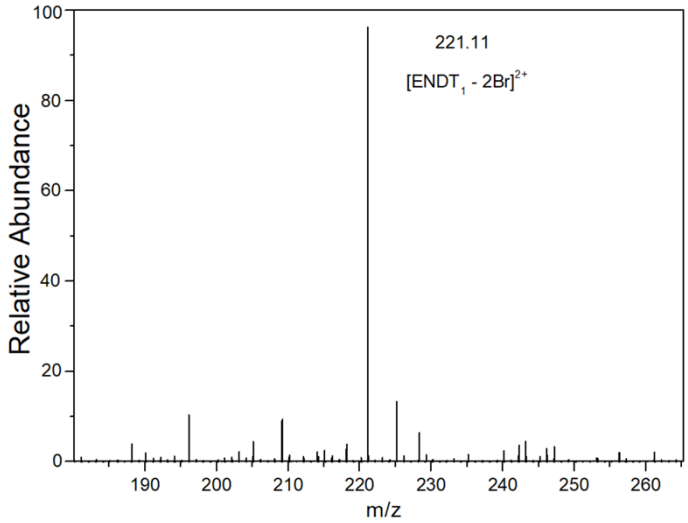

Figure S3. LRMS spectra of $ENDT_1$. Calcd. For C32H30N2 ($[M - 2Br]^{2+}$): 221.12, found: 221.11.

$ENDT_3$: Red solid, 55 %; m.p. > 250 °C. ^1H NMR (400 MHz, $CDCl_3$) δ (ppm): 8.64 (s, 4H), 8.31 (d, J = 8.0 Hz, 2H), 8.12 (s, 4H), 7.99 (s, 4H), 7.48 (s, 4H), 6.92 (d, J = 8.0 Hz, 2H), 4.47 (s, 4H), 1.93 (s, 4H), 1.31 (m, 4H), 0.90 (d, J = 4.0 Hz, 6H). ^{13}C NMR (100 MHz, CD_3CN/DMSO) δ (ppm): 152.9, 144.9, 138.5, 133.1, 132.4, 129.4, 126.9, 126.5, 125.2, 60.5, 33.2, 19.2, 13.4. IR(KBr) υ: 3464, 3392, 3041, 2963, 2882, 1634, 1604, 1510, 1455, 1379, 1311, 1167, 1094, 988, 844, 755 cm^{-1}. LRMS spectra of $ENDT_3$. Calcd. For C36H38N2 ($[M - 2Br]^{2+}$): 249.15, found: 249.13.

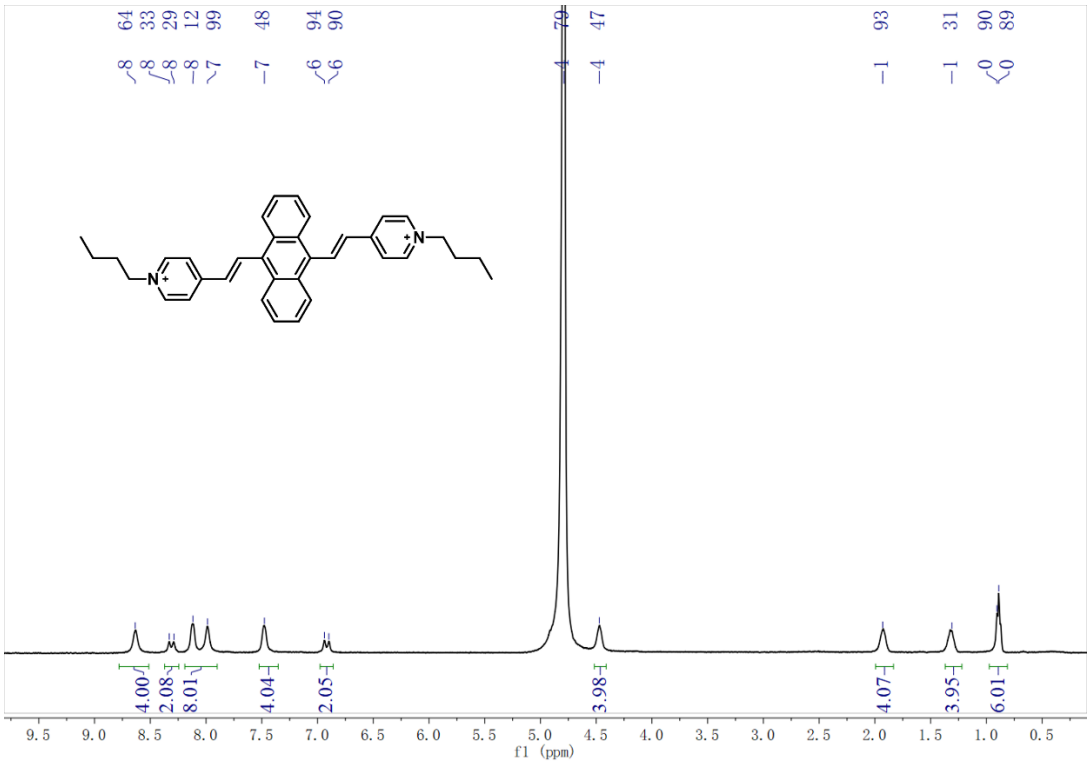

Figure S4. ^{1}H NMR spectra (400 MHz, 298 K, D_2O) of compound $ENDT_3$.

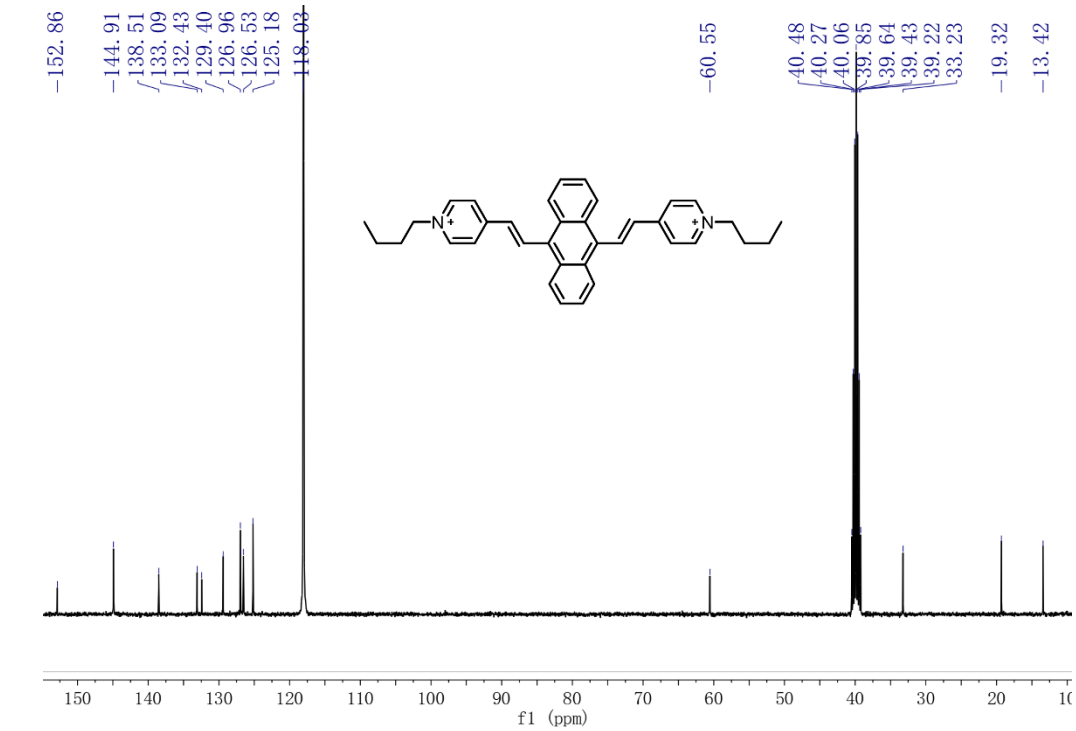

Figure S5. ^{13}C NMR spectra (100 MHz, 298 K, CD_3CN/DMSO) of compound $ENDT_3$.

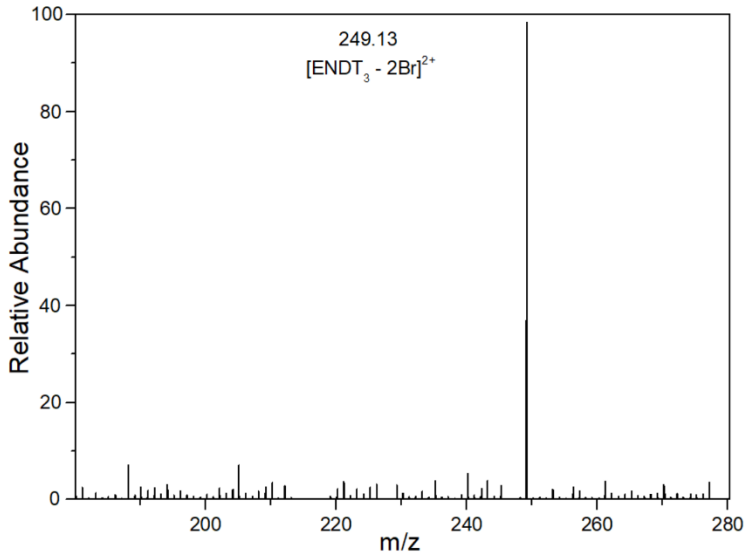

Figure S6. LRMS spectra of $ENDT_3$. Calcd. For C36H38N2 ($[M - 2Br]^{2+}$): 249.15, found: 249.13.

$ENDT_5$: Red solid, 52 %; m.p. > 250 °C. ^{1}H NMR (400 MHz, Acetonitrile-d3) δ (ppm): 8.74 (d, J = 8.0 Hz, 2H), 8.69 (d, J = 4.0 Hz, 4H), 8.41-8.38 (m, 4H), 8.25 (d, J = 4.0 Hz, 4H) 7.64-7.61 (m, 4H), 7.23 (d, J = 8.0 Hz, 4H), 4.51 (t, J = 8.0 Hz, 4H), 2.00 (t, J = 8.0 Hz, 4H), 1.36 (s, 12H), 0.91 (t, J = 6.0 Hz, 6H). ^{13}C NMR (100 MHz, Acetonitrile-d3) δ (ppm): 153.4, 144.8, 138.8, 133.1, 132.5, 129.7, 127. 2, 126.6, 125.4, 118.4, 61.6, 31.3, 25.8, 22.7, 13.8. IR(KBr) υ: 3462, 3385, 3037, 2956, 2927, 2867, 1611, 1508, 1457, 1440, 1258, 1164, 1092, 1015, 858, 799, 743 cm^{-1}. LR-MS spectra of $ENDT_5$. Calcd. For C40H46N2 ($[M - 2Br]^{2+}$): 277.18, found: 277.16.

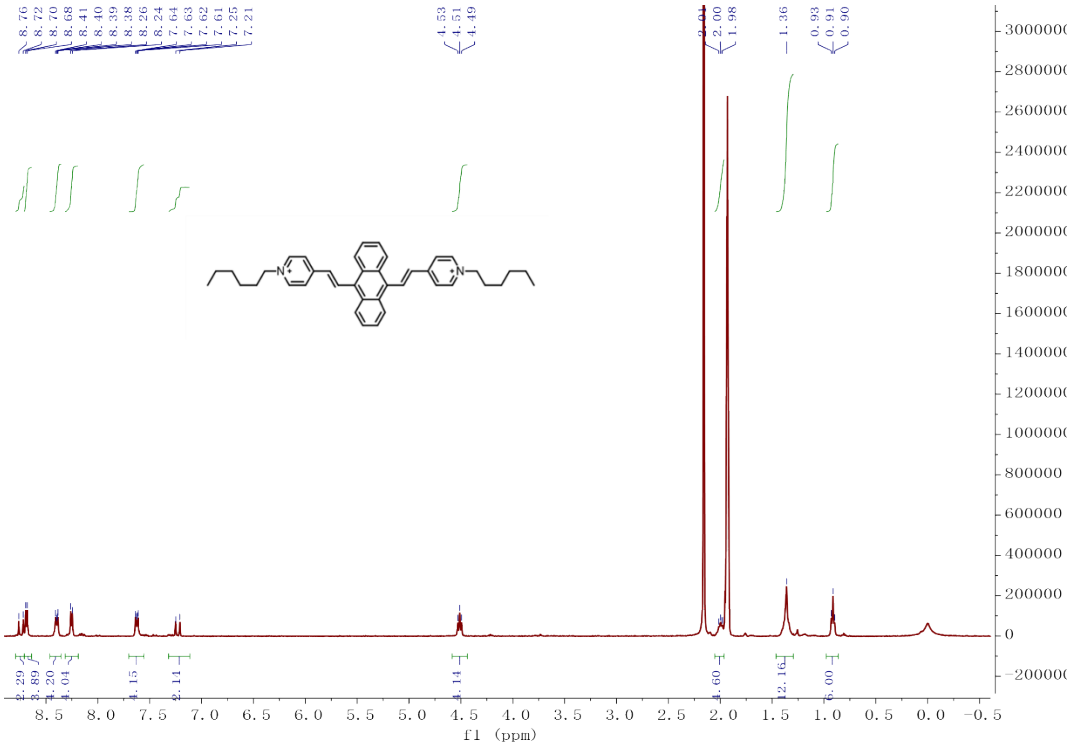

Figure S7. ^{1}H NMR spectra (400 MHz, 298 K, CD_3CN) of compound $ENDT_5$.

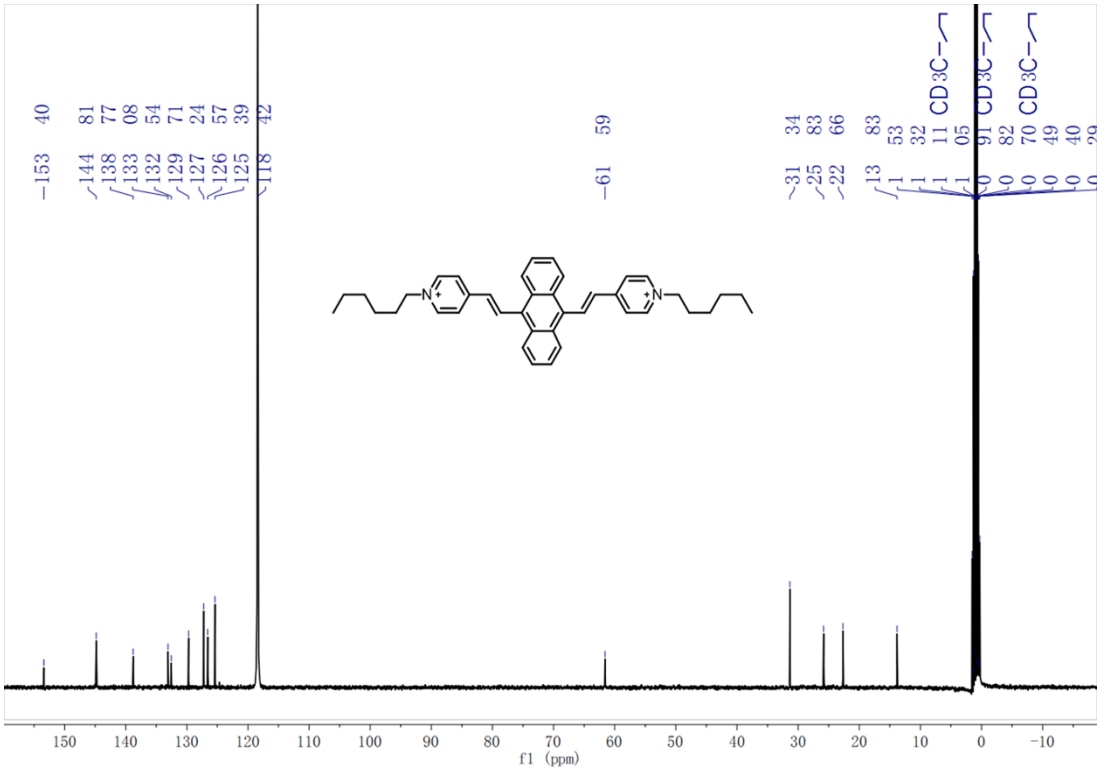

Figure S8. ^{13}C NMR spectra (100 MHz, 298 K, CD_3CN) of compound $ENDT_5$.

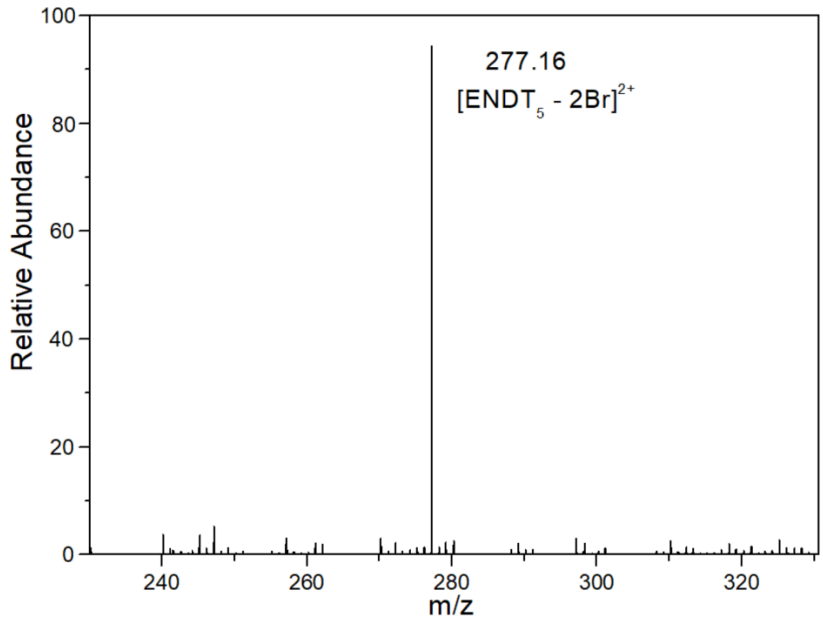

Figure S9. LRMS spectra of $ENDT_5$. Calcd. For C40H46N2 ($[M - 2Br]^{2+}$): 277.18, found: 277.16.

$ENDT_9$: Dark red solid, 49 %; m.p. > 250 °C. ^{1}H NMR (400 MHz, Acetonitrile-d_3) δ (ppm): 8.78 – 8.74 (m, 4H), 8.37 (d, J = 4.0 Hz, 4H), 8.28 (d, J = 8.0 Hz, 2H), 7.63 (t, J = 4.0 Hz, 2H), 7.52 (s, 6H), 7.22 (d, J = 8.0 Hz, 2H), 4.55 (t, J = 8.0 Hz, 4H), 3.44 (t,

J = 6.0 Hz, 4H), 1.39-1.21 (m, 28H), 0.88 (m, 6H). ^{13}C NMR (100 MHz, Acetonitrile-d_3) δ (ppm): 153.4, 144.8, 138.8, 133.1, 132.5, 129.7, 127.2, 126.5, 125.3, 118.5, 61.6, 33.3, 32.1, 31.3, 29.6, 29.1, 26.1, 22.9, 19.5, 13.9, 13.3. IR(KBr) υ: 3440, 3024, 2914, 2846, 1606, 1513, 1457, 1376, 1321, 1164, 1101, 981, 846, 757 cm^{-1}. LRMS spectra of ENDT$_9$. Calcd. For C48H62N2 ([M – 2Br]$^{2+}$): 333.24, found: 333.28.

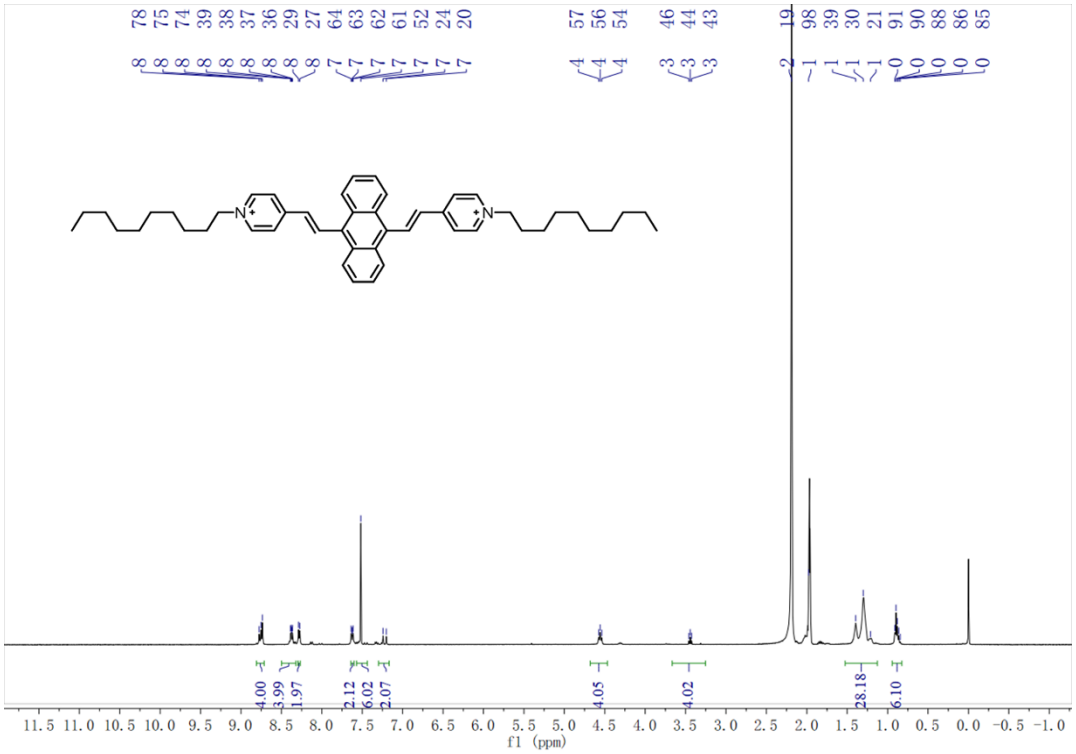

Figure S10. ^{1}H NMR spectra (400 MHz, 298 K, CD_3CN) of compound ENDT$_9$

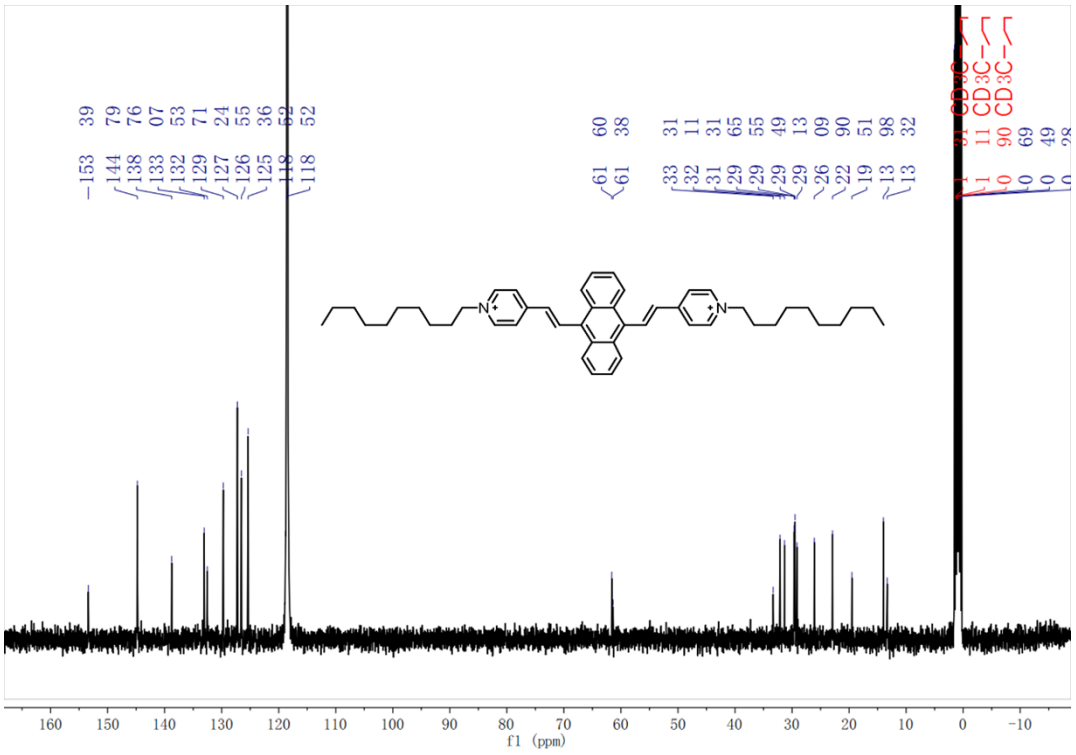

Figure S11. ^{13}C NMR spectra (100 MHz, 298 K, CD_3CN) of compound $ENDT_9$.

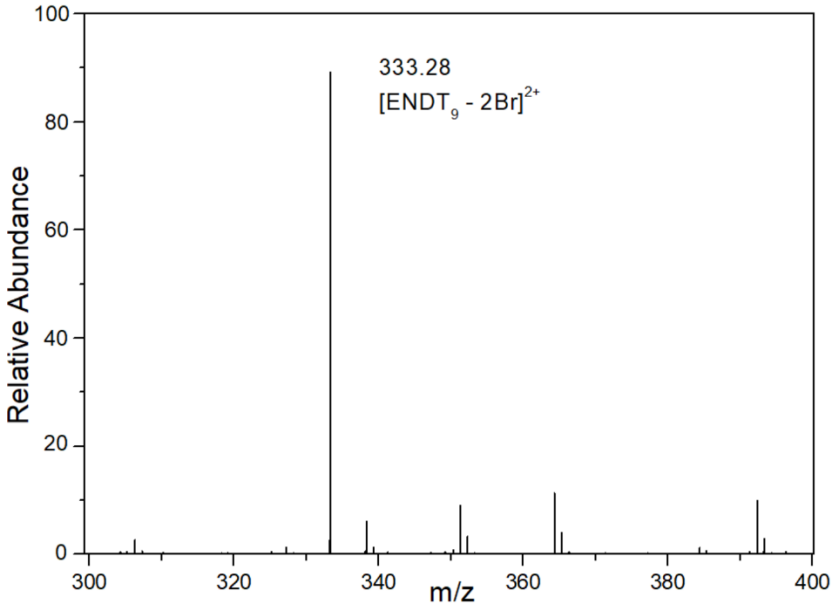

Figure S12. LRMS spectra of $ENDT_9$. Calcd. For C48H62N2 ($[M - 2Br]^{2+}$): 333.24, found: 333.28.

3. Synthesis of **WP5**

WP5 was prepared according to previous report,[S1,S2] and the ^1H NMR was showed in Figure S13.

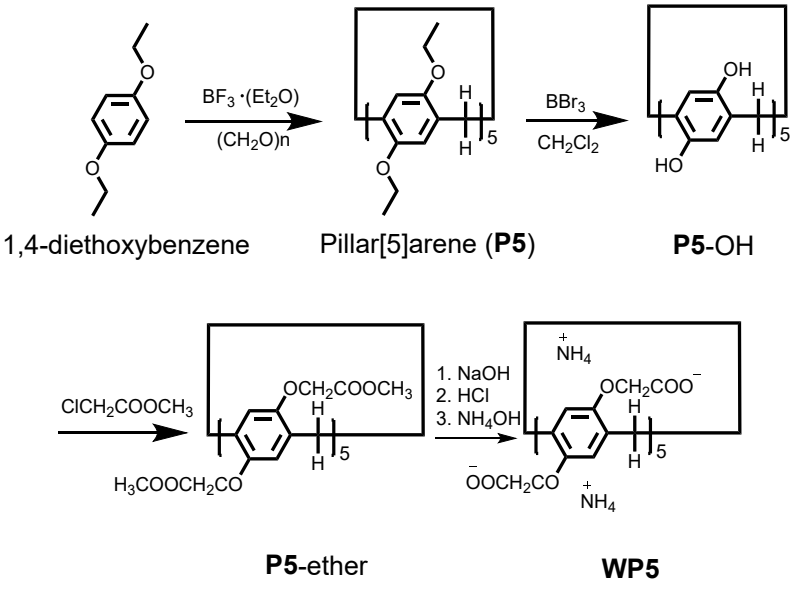

Scheme S2. Synthesis of water soluble pillar[5]arene (**WP5**).

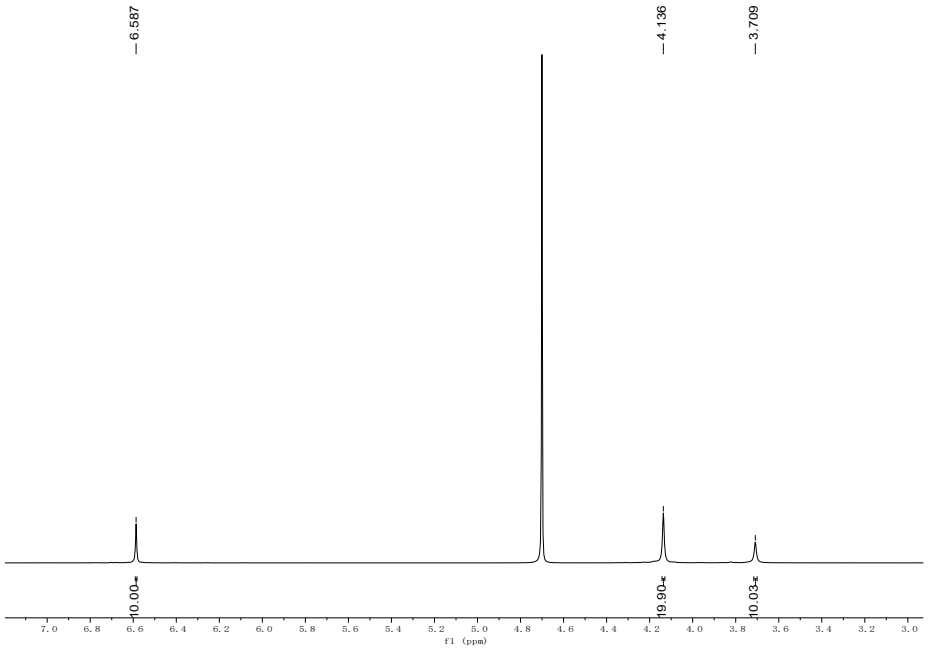

Figure S13. ^{1}HNMR (400 MHz, 298K, D_2O) spectrum of **WP5**.

4. Host-guest interaction between **WP5** and **ENDTn**

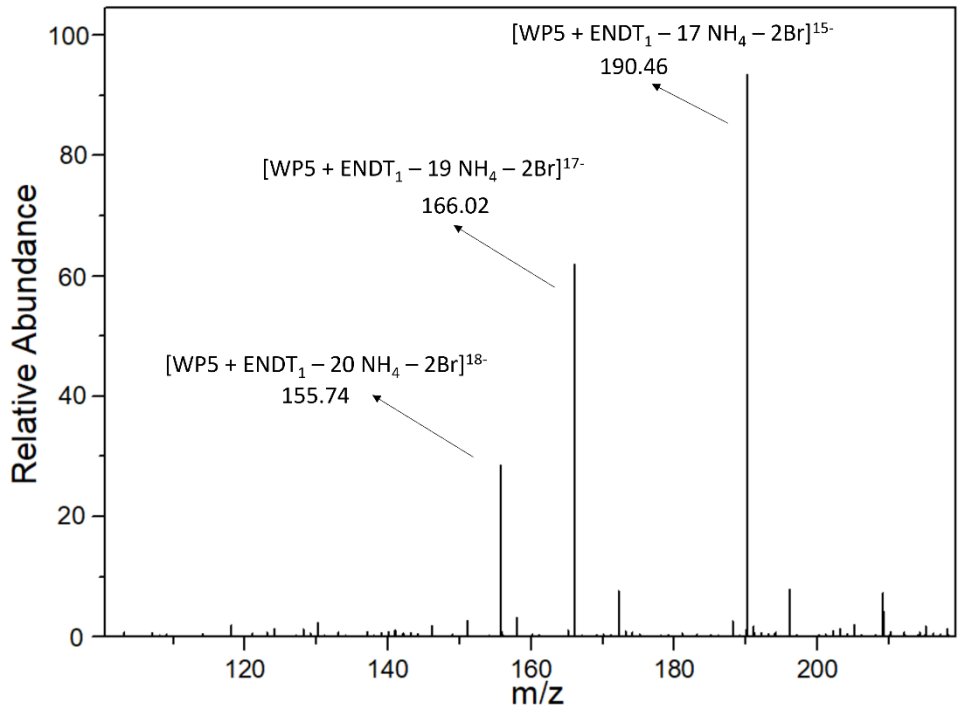

Figure S14. LR-ESI-MS spectra of (WP5)2⊃ENDT$_1$. Calcd. For C142H110N2O60 ([2WP5 + ENDT$_1$ – 20NH$_4$ – 2Br]$^{18-}$): 155.75, found: 155.74; C142H114N3O60 ([2WP5 + ENDT$_1$ – 19NH$_4$ – 2Br]$^{17-}$): 165.98, found: 166.02; C142H122N5O60 ([2WP5 + ENDT$_1$ – 17NH$_4$ – 2Br]$^{15-}$): 190.51, found: 190.46.

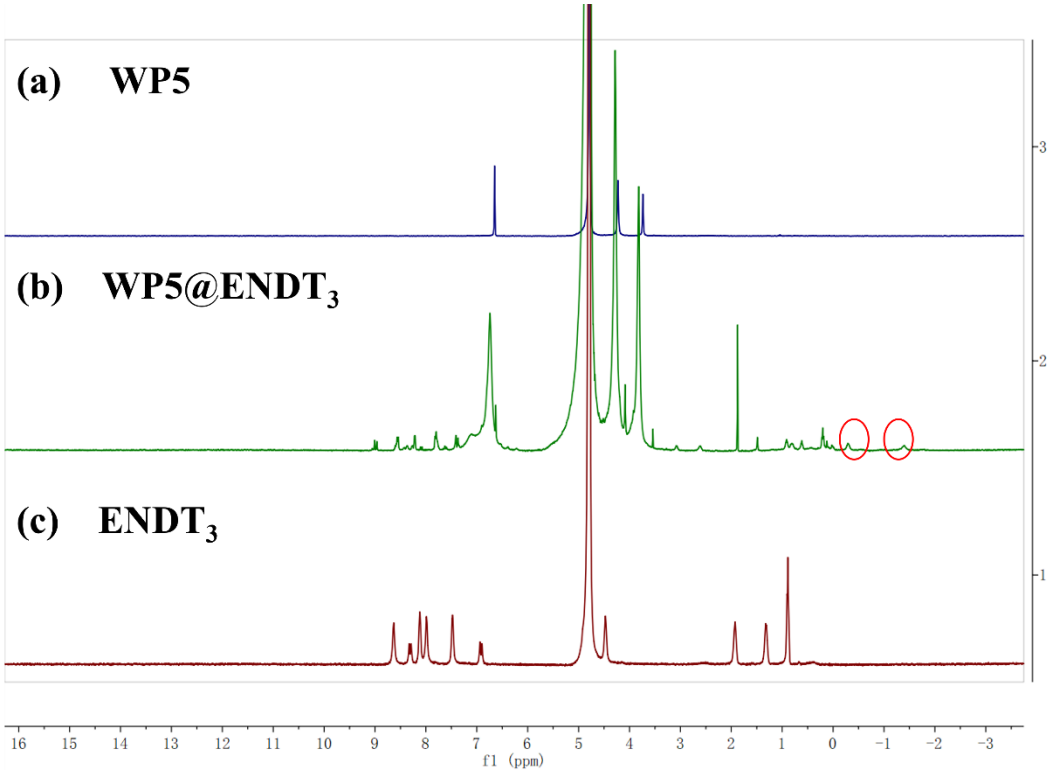

Figure S15. ^{1}H NMR spectra (400 MHz, D_2O, 298 K) of (a) $ENDT_3$ (5.0 mM), (b) $ENDT_3$+WP5 ([$ENDT_3$] = 5.0 mM, [WP5] = 10.0 mM), and (c)$ENDT_3$ (10.0 mM).

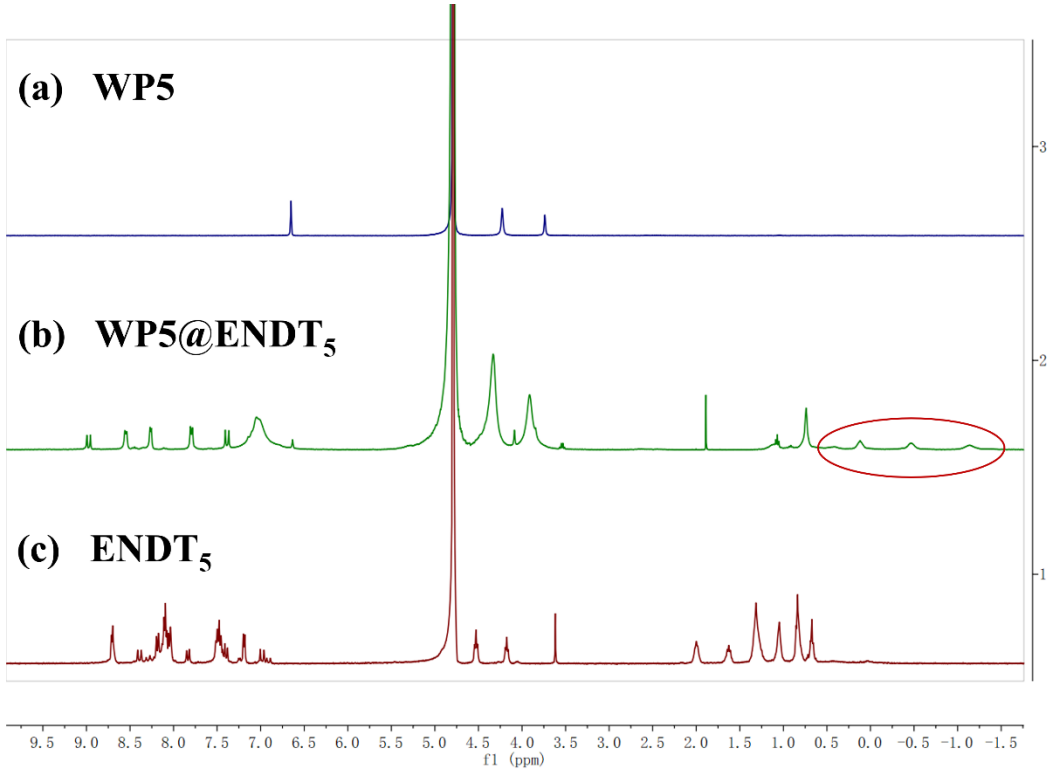

Figure S16. ^{1}H NMR spectra (400 MHz, D_2O, 298 K) of (a) $ENDT_5$ (5.0 mM), (b) $ENDT_5$ + WP5 ([$ENDT_5$] = 5.0 mM, [WP5] = 10.0 mM), and (c)$ENDT_5$ (10.0 mM).

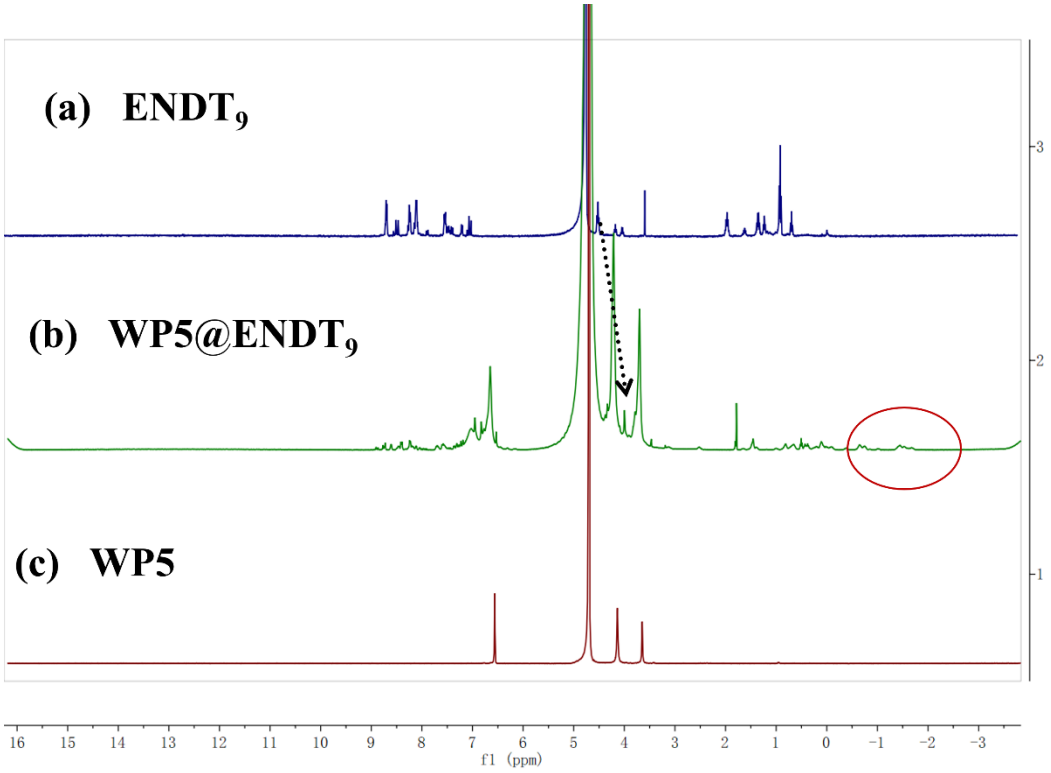

Figure S17. ^{1}H NMR spectra (400 MHz, D_2O, 298 K) of (a) $ENDT_9$ (5.0 mM), (b) $ENDT_9$ + WP5 ([$ENDT_9$] = 5.0 mM, [WP5] = 10.0 mM), and (c) $ENDT_9$ (10.0 mM).

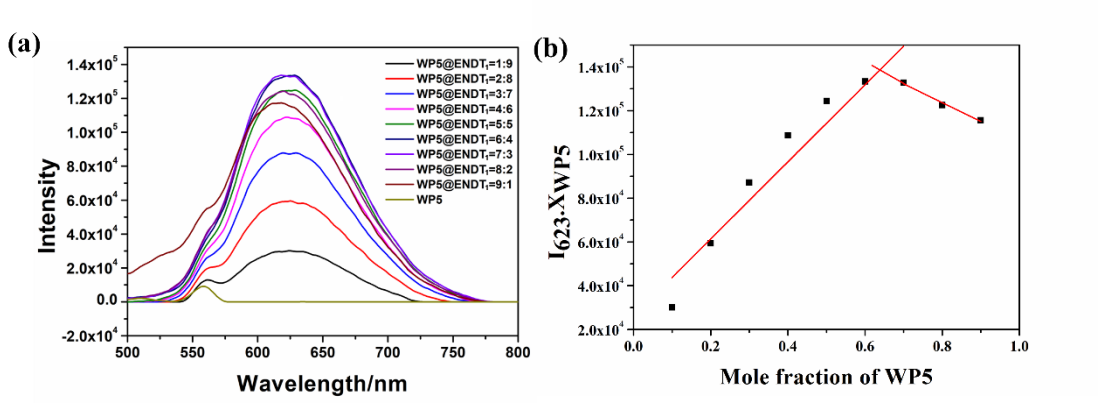

Figure S18. (a) Fluorescence titration of $ENDT_1$ (10 μM) with different concentration of WP5. (b) (B) Job's plot for $ENDT_1$ upon addition of WP5 in aqueous medium ([$ENDT_1$] + [WP5] = 10 μM]).

5. Self-assembly properties

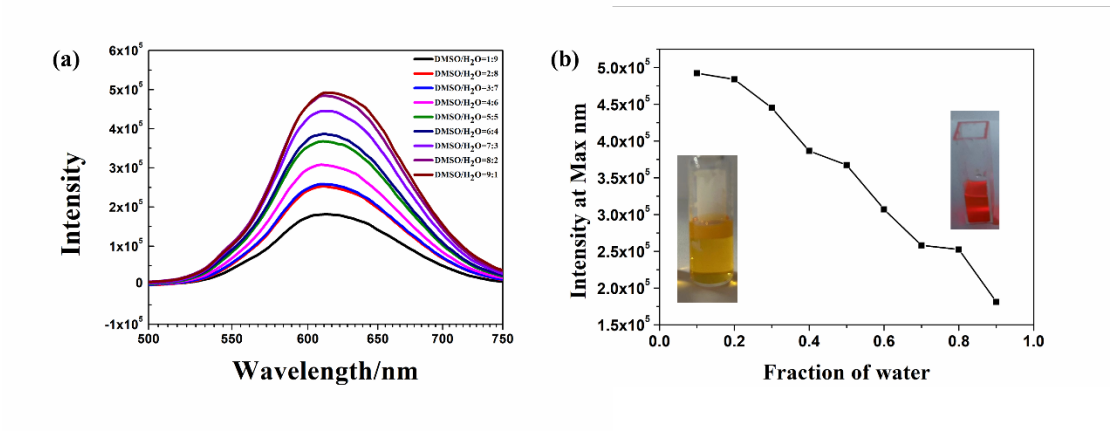

Figure S19. (a) Fluorescence emission of $ENDT_1$ (10 μmol/L) in different ratio of H_2O/DMSO mixture. (b) Fluorescence emission of $ENDT_1$ (10 μmol/L) in Max ratio of H_2O/DMSO mixture.

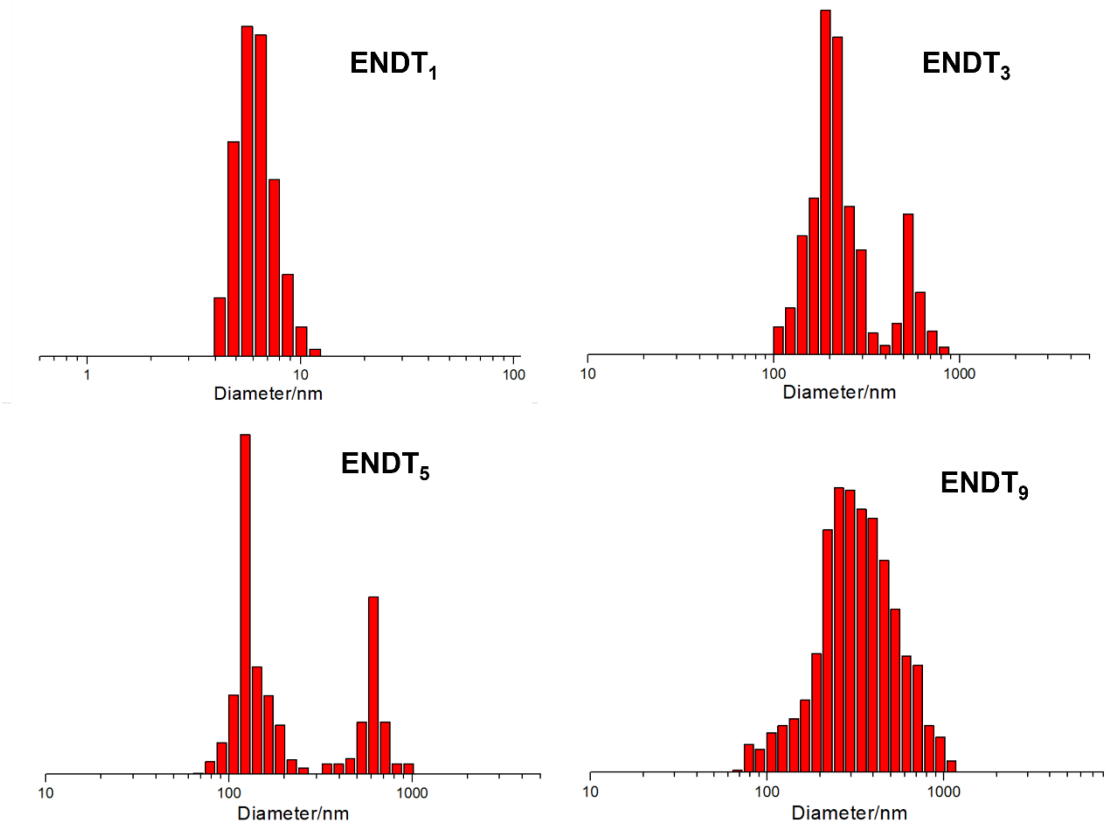

Figure S20. DLS data of $ENDT_n$ (10 μmol/L) in water.

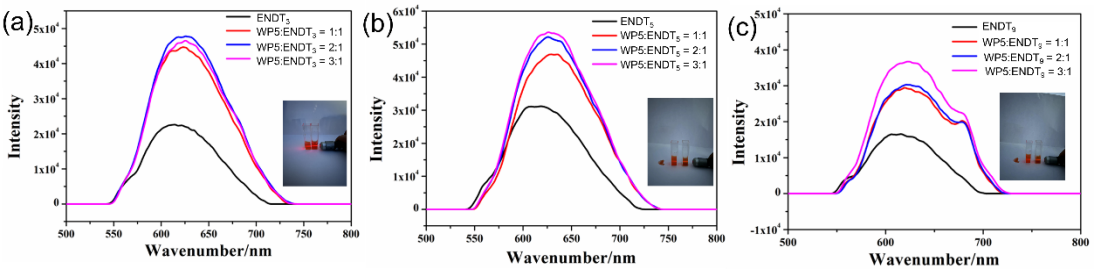

Figure S21. (a-c) Fluorescence titration of $ENDT_3$, $ENDT_5$, $ENDT_9$ (10 μM) with different concentration of WP5. λ_{ex} = 470 nm. Insert: Trndall of $ENDT_3$, $ENDT_5$, $ENDT_9$ and WP5@$ENDT_3$, WP5@$ENDT_5$, WP5@$ENDT_9$.

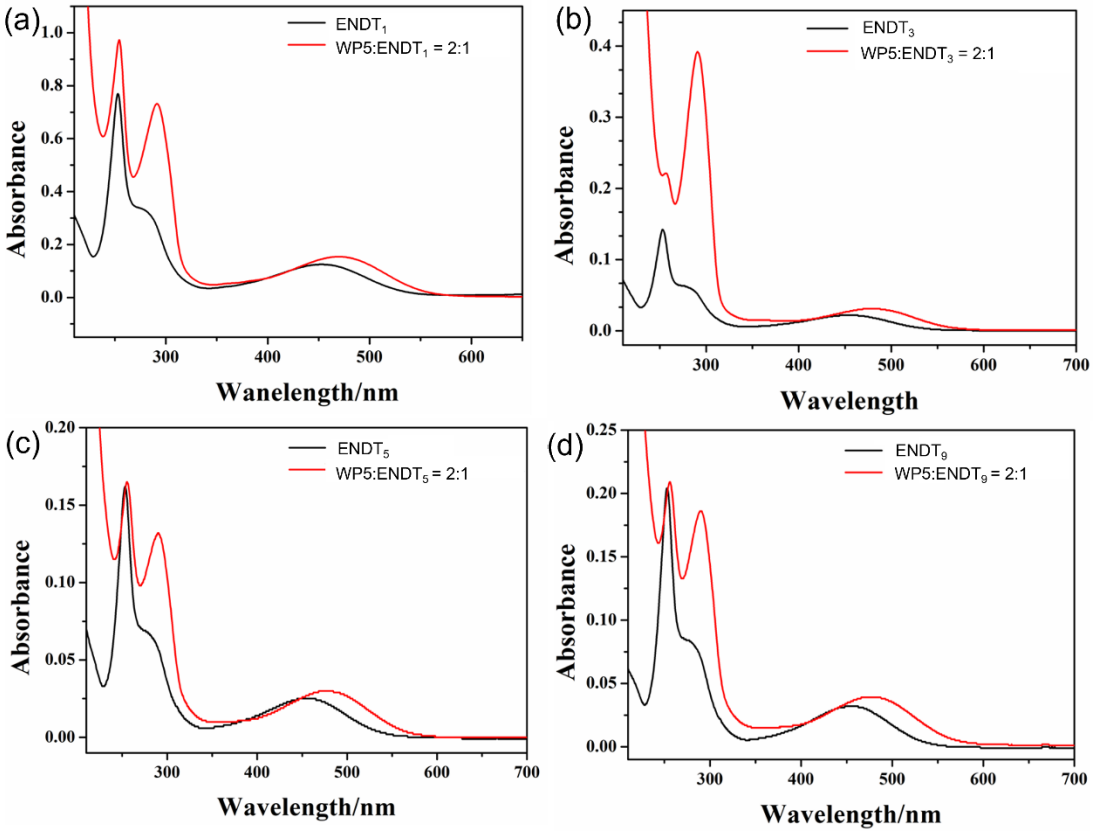

Figure S22. (a-d) UV–vis absorption spectra of ENDT-(1,3,5,9) and $(WP5)_2$@ENDT-(1,3,5,9). [ENDT-(1,3,5,9) = 10 μmol/L, WP5 = 20 μmol/L].

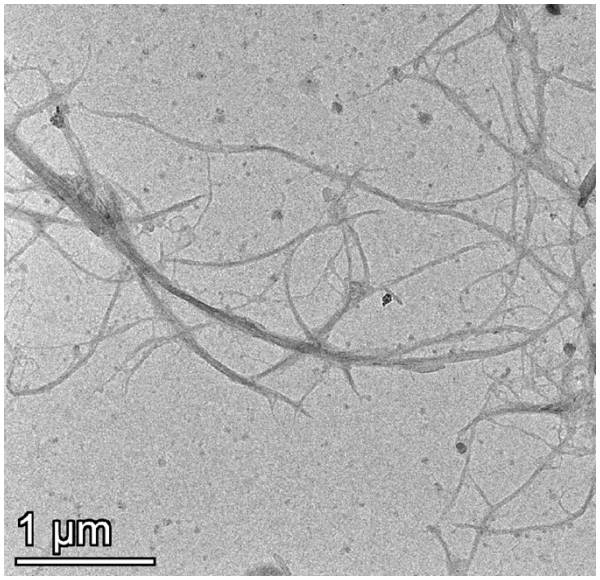

Figure S23. TEM image of $ENDT_9$ based assemblies in water.

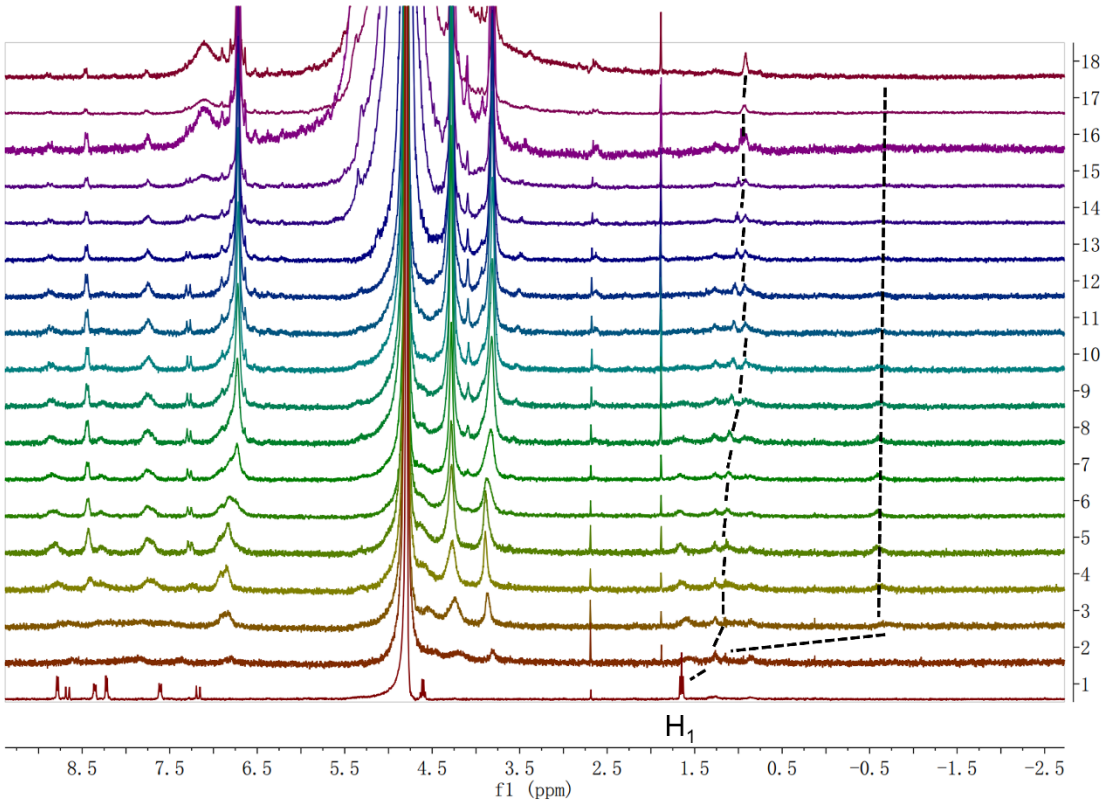

Fig. S24. ^1H NMR spectra (400 MHz,D_2O, 298 K) of $ENDT_1$ at a concentration of 1.00 mM upon addition of various concentrations of the molecular WP5: (1) 0 mM, (2) 0.196 mM, (3) 0.385 mM, (4) 0.566 mM, (5) 0.741 mM, (6) 0.909 mM, (7) 1.228 mM, (8) 1.525 mM, (9) 1.803 mM, (10) 2.063mM, (11) 2.308 mM, (12) 2.537 mM, (13) 2.754 mM, (14) 2.966 mM, (15) 3.151 mM, (16) 3.590 mM, (17) 3.976 mM and (18) 4.318 mM.

The non-linear curve-fitting was based on a previous report.[S3]

$$\Delta\delta = (\Delta\delta_{\infty}/[G]_0)\,(0.5[H]_0 + 0.5([G]_0+1/K_a) - (0.5\,([H]_0^2 + (2[H]_0\,(1/K_a - [G]_0)) + (1/K_a + [G]_0)^2)^{0.5})) \quad \text{(Eq. S1)}$$

where $\Delta\delta$ is the chemical shift change of H_1 on $ENDT_1$, $\Delta\delta_{\infty}$ is the chemical shift change of H_1 when $ENDT_1$ is completely complexed, $[H]_0$ is the initial concentration of the WP5, and $[G]_0$ is the fixed initial concentration of $ENDT_1$.

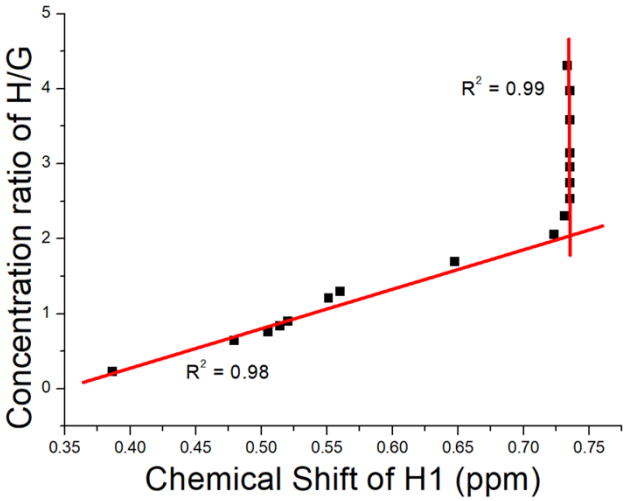

Fig. S25 Mole ratio plot for **WP5** and ENDT1, indicating a 2 : 1 stoichiometry.

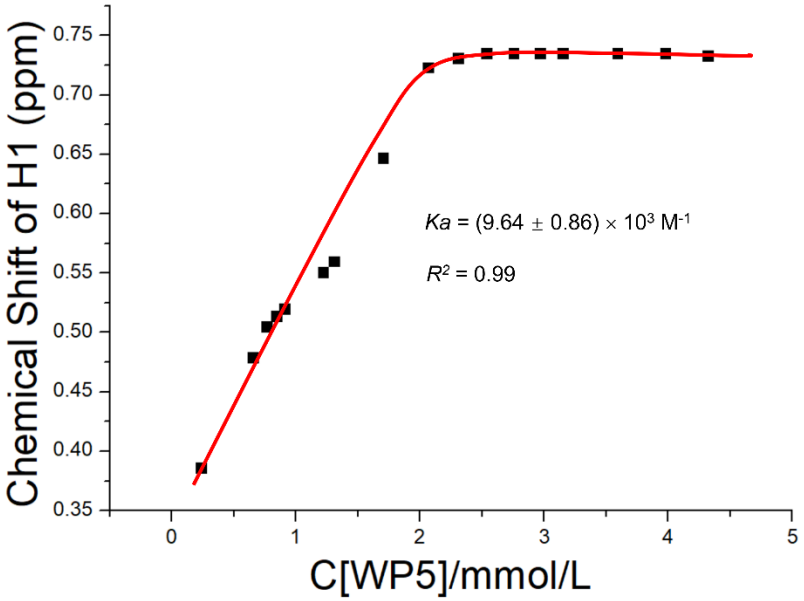

Fig. S26. The chemical shift changes of H_1 on ENDT1 upon addition of **WP5**. The red solid line was obtained from the non-linear curve-fitting.

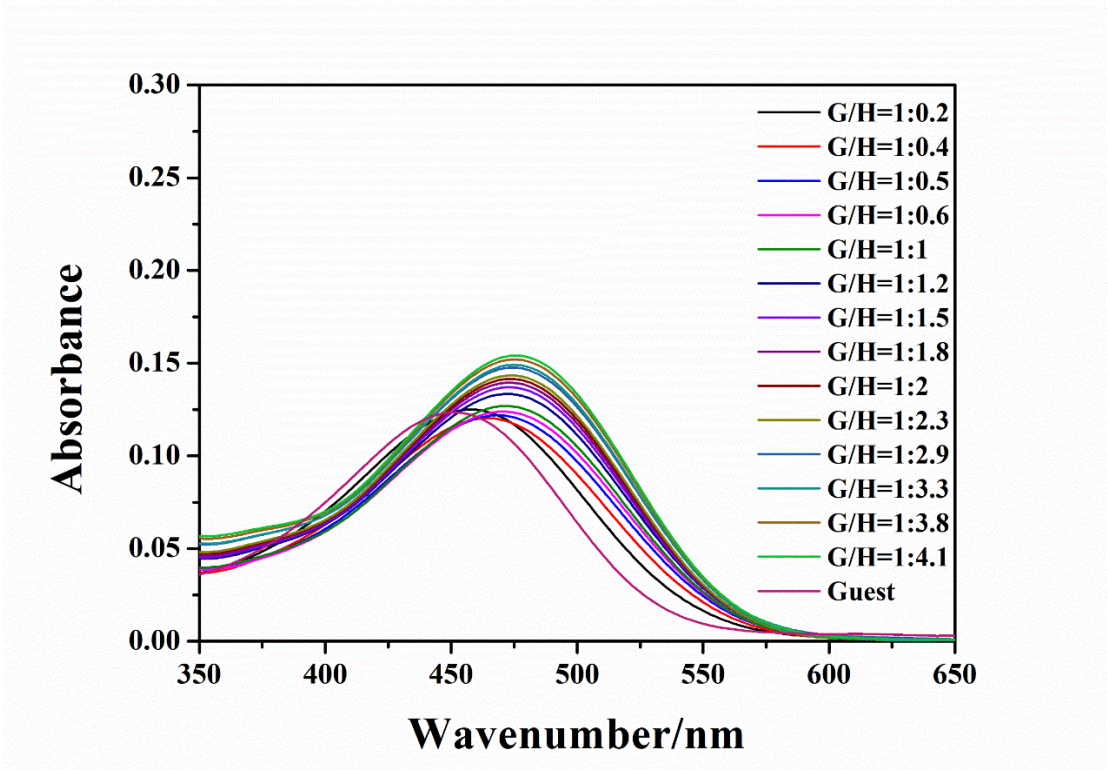

Fig. S27 UV-Vis titration of ENDT (10 μm) upon addition of WP5.

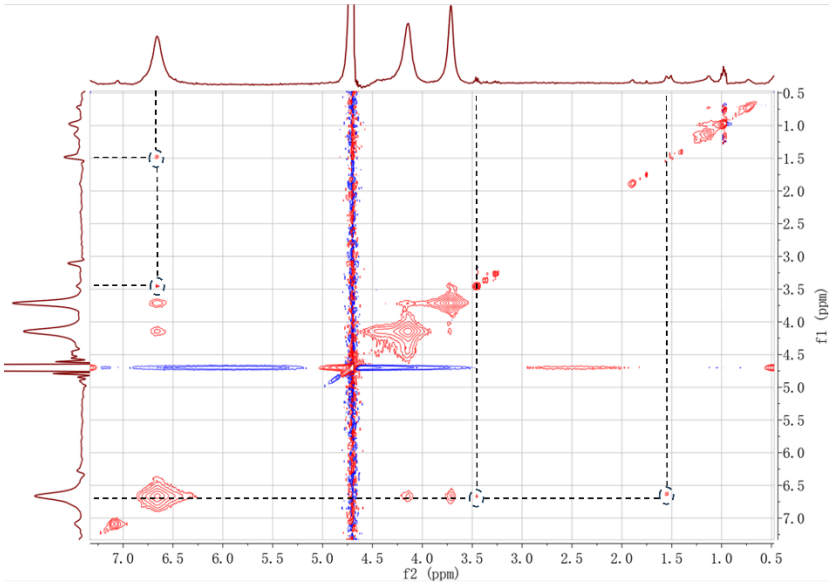

Fig. S28. 2D NOE NMR spectrum (400 MHz, D_2O, 298 K) of $(WP5)_2 \supset ENDT_1$ at 1.0 mM.

6. References

S1. Tomoki Ogoshi, Masayoshi Hashizume, Tada-aki Yamagishi and Yoshiaki

Nakamoto, *Chem. Commun.*, **2010,** *46*, 3708-3710.

S2. Yue Zhang, Yang Wang, Tingting Chen, Ying Han, Chaoguo Yan, Jin Wang, Bing Lu, Longtao Ma, Yue Ding, and Yong Yao, *Chem. Commun.*, **2023**, *59*, 8266-8269.

S3. P. R. Ashton, R. Ballardini, V. Balzani, M. Bělohradský, M. T. Gandolfi, D. Philp, L. Prodi, F. M. Raymo, M. V. Reddington, N. Spencer, J. F. Stoddart, M. Venturi, D. J. Williams. *J. Am. Chem. Soc.* **1996**, *118*, 4931–4951.